Quantitative Investigation of the Radiation of the Negative Iodine Ion +

Manfred Neiger *

Elektrophysikalisches Institut der Technischen Universität München **

(Z. Naturforsch. **30 a**, 474–484 [1975]; received January 17, 1975)

A pure iodine plasma is generated by a cylindric arc at 1 atm and 6 to 30 amps within a quartz tube of 8 mm diameter. The radiation emitted along the arc axis was measured absolutely in the wavelength range from 0.2–1.9 μ. In the uv-region it consists mainly of the affinity continuum due to transitions of free electrons to the ground level of the negative iodine ions. The first threshold of this continuum at 4048 Å yields an electron affinity of the iodine atom of 3.062 eV. The resulting photodetachment cross-section of the I^--ion exhibits a broad peak at 2400 Å, which can be attributed to a I^--compound-state. The continuous background radiation in the visible and infrared regions shows, after subtraction of the electron-ion continuum, two long-wavelength thresholds near 1.25 μ and 0.64 μ. The absolute intensity of this radiation, its wavelength and temperature dependence and its threshold energy and threshold structure suggest the contribution of two dominant radiation processes: a second affinity continuum due to an excited state of the I^--ion about 2 eV above the ground level and an association continuum of I_2^+-molecules. Towards longer wavelengths $\lambda > 1.5$ μ electron-atom Bremsstrahlung becomes more important.

Introduction

Halogens are especially suitable for the investigation of radiation processes of negative ions, because of their large electron affinity [1] (3.0 – 3.6 eV) and the consequently conveniently accessible spectral region for spectroscopic investigations. Halogen plasmas of a high degree of dissociation and a low degree of ionisation strongly emit a so-called affinity continuum in the uv-region, which is generated by radiative attachment of free electrons to neutral halogen atoms. The electron affinities of these elements can be determined very accurately and easily from the continuum thresholds [1]. The photodetachment cross-section of the negative ions as a function of wavelengths results from an absolute continuum measurement together with a determination of the temperature of the radiating plasma. The electron affinities and detachment cross-sections of the halogens fluorine [2], chlorine [3], and bromine [4] have been determined by this method using a wall-stabilized low current arc plasma. From measurements at shock-heated plasmas containing fluorine, chlorine, bromine and iodine [5–7], the same quantities have been determined. These experimental results show good agreement with each other, as well as compared with theoretical calculations of detachment cross-sections by Robinson and Geltman [8].

In addition to the affinity continuum in the uv-region, an intense visible continuum was found to be emitted from low-current arcs operated in pure chlorine [3] and bromine [4] vapours, which could not be interpreted as electron-ion bremsstrahlung according to Kramers/Unsöld [9, 10] and Maecker/Peters [11]. The following radiation processes have been proposed as alternative explanations:

- electron-atom bremsstrahlung (so called free-free-minus continuum) [4, 12],
- radiative recombination of a neutral atom and a positive ion to form a positive molecular ion (so-called association continuum) [13].

This article reports on a quantitative measurement of the radiation of a pure iodine plasma with negative iodine ions playing a dominant part. An attempt is also made towards a further understanding of the visible continuum by extending the spectroscopic measurements to the near infrared region.

+ This work forms part of a thesis submitted to the "Fakultät für Maschinenwesen und Elektrotechnik der Technischen Universität München" in partial fulfillment of the requirements for the degree of Dr.-Ing.

Acknowledged on February 28, 1974.

* Present address: Department of Physics and Astronomy, University of Maryland, College Park, Maryland 20742, USA.

** Reprint requests to Prof. Dr. H. Maecker, Elektrophysikalisches Institut der TU München, *D-8000 München 2*, Arcisstrasse 21, West Germany.

1. Measurements

1.1. Iodine Arc

A schematic drawing of the arc apparatus is shown in Figure 1. The wall-stabilized arc is operated at atmospheric pressure. The center plasma column, burning in pure iodine vapour, is electrically connected to the electrodes by short argon

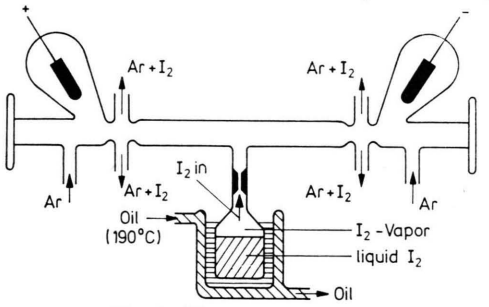

Fig. 1. The arc apparatus.

arcs. Iodine vapour flowing from the center and argon gas flowing from the electrode regions towards both outlets prevent mixing of these gases within the plasma column. Besides protecting the electrodes, this configuration generates an axially homogenous iodine plasma column, which can be spectroscopically investigated end-on through transparent, negligibly self-radiating "argon-windows".

The iodine flow is generated by evaporation from the surface of liquid iodine, heated up to 190 °C in a thermostatically controlled quartz container. A heated quartz pipe with a narrow capillary provides the connection to the arc vessel. A temperature control better than 0.1 °C is necessary to achieve a steady iodine flow into the plasma. With an argon counterflow of 4 cm^3/s on each side, the iodine region is separated from the argon regions by a narrow transition layer of about 1 mm thickness.

To obtain good mechanical, thermal and chemical resistivity of the arc vessel, this is made of quartz glass. The dimensions of the cylindrical center part, in which the pure iodine plasma is generated, are 10 cm length, 8 mm inner diameter and 1 mm wall thickness.

The necessary cooling of the walls of the arc vessel is achieved by blowing high pressure air radially inward onto it. Water cooling is forbidden at the applied currents below 30 amps to prevent condensation and sublimation of iodine vapour at the inner surface of the plasma stabilizing wall.

Under these conditions, a highly stable and reproducible iodine arc is obtained in the current range from 6 to 30 amps. Arc ignition is achieved by a high voltage breakdown in pure argon gas of a few torr pressure.

1.2. Recording of Spectra

The axis of the iodine arc was focussed end-on 1:1 to the entrance slit of a grating double-monochromator by an achromatic quartz lens of 20 cm focal length. A quartz window (Suprasil) sealed the observation end of the arc vessel. A stop in the focal plane between lens and entrance slit limited the solid angles of all rays to 1/200. Only radiation of a homogenous plasma column of constant temperature around the arc axis and of the cross-section of the entrance slit could therefore enter the spectrometer.

Two different gratings, blazed at 5000 and 10,000 Å were used for spectroscopic measurements between 0.2 and 1.9 μ. Glass filters and the selectivity of the different photoelectric radiation detectors eliminated undesired diffraction orders. The following detectors were used:

Wavelength-range	Detector
2000 Å − 3500 Å	PM, EMI 9616 QB (solar-blind)
2500 Å − 7000 Å	PM, EMI 9598 QB (S20)
0.7 μ − 1.1 μ	PM, EMI 9684 QB (S1)
0.7 μ − 1.9 μ	PbS-cell, Valvo 61 SV

The electrical signals were taken from $1-5\,M\Omega$ anode resistors and displayed on a strip-chart recorder. To overcome the high noise levels of both the S1-PM tube and the PbS-cell phase-sensitive detection was employed.

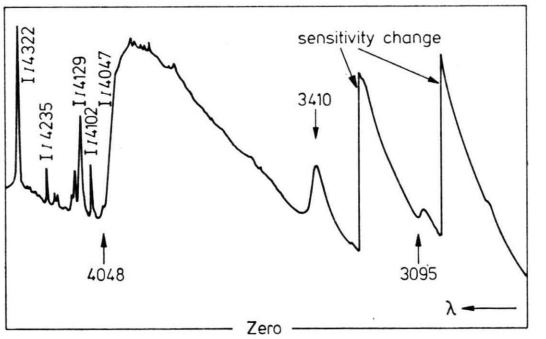

Fig. 2. Photoelectric recording of the ultraviolet spectrum of the iodine arc ($I=20$ amps; wavelengths in Å).

Figure 2 shows an example of a photoelectric recording between 2700 and 4300 Å. The two long wavelength thresholds of the iodine affinity continuum show up very distinctly near 4050 Å and 3100 Å. Figure 3 shows a recording in the vicinity of the first of these thresholds.

1.3. Absolute Spectral Continuum Intensities

The calibration of the measured relative spectral intensities was performed with a standard carbon arc according to Euler [14] and Magdeburg [15] (Anode

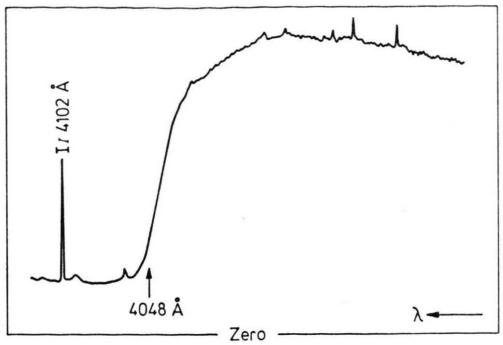

Fig. 3. Photoelectric recording of the spectrum in the vicinity of the first threshold of the uv affinity continuum (I=7 amps).

RW II, 6.35 mm ϕ; 7.3 amps). As Magdeburg's tabulated carbon arc spectral intensities start only at 2500 Å, Pitz's [16] values, which differ at this wavelength only slightly from Magdeburg's, were used between 2000 and 2500 Å.

As we are interested in continuum radiation only, all spectral lines were subtracted from the recordings. In the infrared range, continuum measurements were performed only at discrete wavelengths which were found before to be free of spectral lines over a sufficiently wide interval. Figures 4 and 5 show the results of the measurements from 2000 Å to 1.9 μ for three different arc currents.

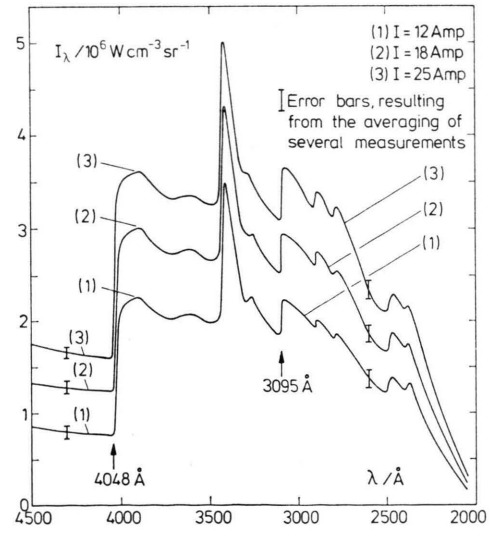

Fig. 4. Absolute spectral μv continuum intensities.

1.4. Plasma Composition

A detailed knowledge of the composition and the temperature of the radiating plasma column is necessary for an evaluation and interpretation of the measured continuum intensities.

The temperature dependent number densities of plasma particles are calculated on the basis of the following equilibrium relations:

1. Dalton's law of partial pressures.
2. Chemical equilibrium law for the dissociation of molecules.
3. Two Saha equations for the ionisation of atoms and negative ions.
4. Quasineutrality condition.

These equations have been solved for a pure iodine plasma using a computer program according to Frie [17] and the following input data:

Dissociation energy of $I_2 = 1.54$ eV,
Ionisation energy of $I = 10.45$ eV,
Electron affinity of $I = 3.06$ eV,
Constant arc pressure $p = 0.97$ atm.

The partition functions of the iodine molecule and atom were calculated on the basis of term values from Herzberg [18] and Moore [19]. The negative iodine ion's partition function has been assumed to be one. Figure 6 shows the resulting particle number densities as a function of plasma temperature in the range 3500 – 8500 K.

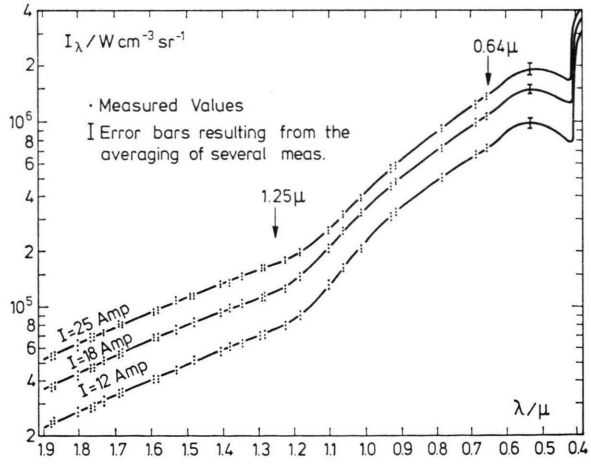

Fig. 5. Absolute spectral ir continuum intensities.

1.5. Temperature Determination

The determination of the temperature of the axis of the iodine plasma column suffered from the lack of transition probabilities for iodine spectral lines. Using a computer program of Friedrich and Trefftz, which is based on the Coulomb approximation method [20, 21], transition probabilities for the following three I_I-lines have been calculated:

Line (Å)	Transition $(n) - (m)$	Transition probability (calculated) A_{nm} (10^6 s^{-1})
4763	$7p^4P^0_{3/2} - 6s^4P_{5/2}$	3.45
4862	$7p^4D^0_{7/2} - 6s^4P_{5/2}$	3.82
5764	$6p^4D^0_{3/2} - 6s^4P_{5/2}$	1.06

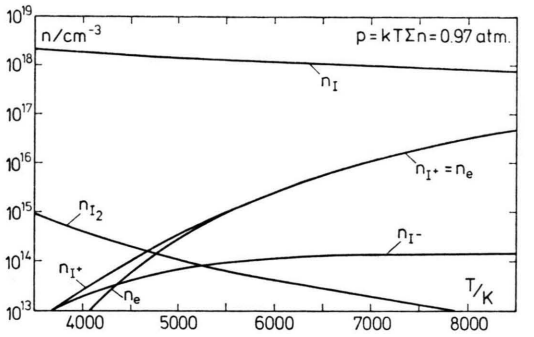

Fig. 6. Particle number densities of the iodine plasma.

Assuming optically thin emission, which was checked and found valid, an absolute measurement of the integrated intensities of these lines for different arc currents yielded the axis temperature as a function of arc current. Figure 7 shows that these values differ by no more than ± 30 K.

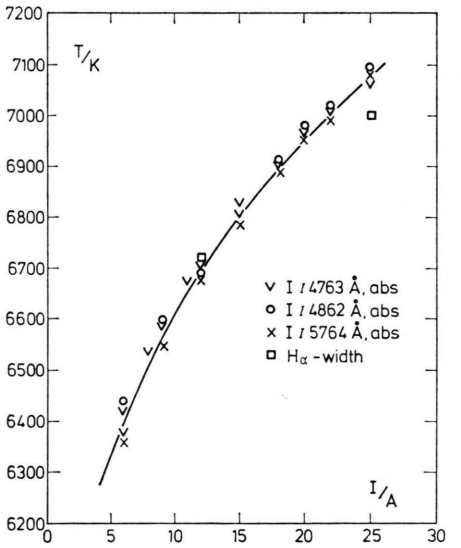

Fig. 7. Axis temperature of the iodine arc as function of current.

As a check of these temperature measurements, which are based upon approximately calculated transition probabilities, the electron density was determined from the half-width of the hydrogen H_α line by adding very small amouts of hydrogen to the iodine plasma column. H_β could not be used as an electron density probe because of the very strong nearby I_I 4862 line. Electron density is related to the plasma temperature via the particle density graph. Figure 7 shows that the former temperature determination is reasonably confirmed by this check.

The following evaluations use the plasma temperatures 6700 K for $I = 12$ amps, 6900 K for $I = 18$ amps, and 7070 K for $I = 25$ amps.

2. Analysis of the UV-Continuum

2.1. Electron Affinity of Iodine

The electron affinity of the iodine atom can be determined directly from the registered traces of the uv-continuum (see Figs. 2 and 3). The continuum thresholds at $\lambda_1 = 4048$ Å and $\lambda_2 = 3095$ Å belong to the iodine affinity continuum and mark the onset of radiative attachment of free electrons to the iodine ground levels $^2P^0_{3/2}$ and $^2P^0_{1/2}$. The threshold wavelengths are determined by using a procedure proposed by Berry [22]. This method yields the following threshold wavelengths and corresponding energies:

1. threshold: (4048 ± 2) Å or (3.062 ± 0.002) eV,
2. threshold: (3095 ± 5) Å or (4.005 ± 0.007) eV.

No shift of these thresholds with temperature could be observed, but increasing temperature, which means increasing electron density, yields increasing smear out. The difference of 0.943 eV of these thresholds coincides with the ground state splitting of the iodine atom within experimental error.

These values yield an electron affinity of iodine of $EA(I) = (3.062 \pm 0.002)$ eV.

The long wavelength threshold of the iodine affinity continuum was also measured using shock-heated plasmas. Rothe [16] reported the value 3.059 eV from emission measurements, Mandl and Hyman [7] got 3.061 eV with an absorption technique. Our value coincides with these within the experimental errors.

2.2. Absorption Coefficient of the UV-Continuum

The absolute spectral intensities emitted by the arc axis at 6700, 6900, and 7070 K axis temperatures (see Fig. 4) are converted into wavelength dependent absorption coefficients by means of

Kirchhoff's law with induced emission taken into consideration:

$$K(\lambda) = J_\lambda/(l \cdot W_\lambda)$$

l = length of iodine plasma column (10 cm), W_λ = Planck black body intensity function.

The affinity continuum contributes the dominant part by far. Its absorption coefficient $\varkappa_{\text{aff}}$ is related to the ground state $^1S_0$ of the negative iodine ion according to the elementary process

$$I^-(^1S_0) + h\,c/\lambda \rightarrow I(^2P^0) + e[(m/2)\,v^2]\,.$$

It holds therefore

$$\varkappa_{\text{aff}}(\lambda, T) = \sigma_{\text{det}}^{(0)}(\lambda) \cdot n_-^{(0)}(T)$$

$n_-^{(0)}(T)$ = particle number density of I^- ions in the ground state $^1S_0$. $\sigma_{\text{det}}^{(0)}(\lambda)$ = photodetachment cross-section.

The following procedure is adapted to separate this absorption coefficient from the total continuum: An extrapolation of the total absorption coefficient for $\lambda > 4050$ Å to shorter wavelengths separates a temperature dependent part ("U" = background) from the affinity continuum. As a parabolic and an exponential extrapolation do not differ by more than 20%, an average value of both is taken. Then the quantity $(\varkappa_{\text{tot}} - \varkappa_{\text{U}})/n_-^{(0)}$ is calculated, which is plotted in Fig. 8 for the three temperatures involved. It is obvious that it can be considered as being composed of two different contributions, one dependent on and the other independent of temperature. The first one is due to diffuse bands of molecular iodine, which are known in the literature [23, 24] because they appear very strongly in almost all discharges through iodine. The second part, independent of temperature, can be identified with the photodetachment cross-section $\sigma_{\text{det}}^{(0)}(\lambda)$ of the I^- ion in its ground state $^1S_0$.

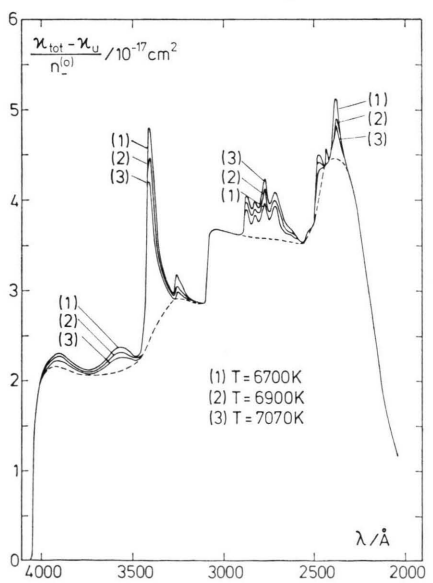

Fig. 8. Evaluation of the photodetachment cross-section of the I^- ground state.

2.3. *Photodetachment Cross-section of the I^- ion in its Ground State*

Figure 9 shows the result for the I^- photodetachment cross-section, evaluated as described in Chapter 2.2. The experimental results of Mandl and Hyman [7] and the theoretical predictions of Robinson and Geltman [8] are included for comparison.

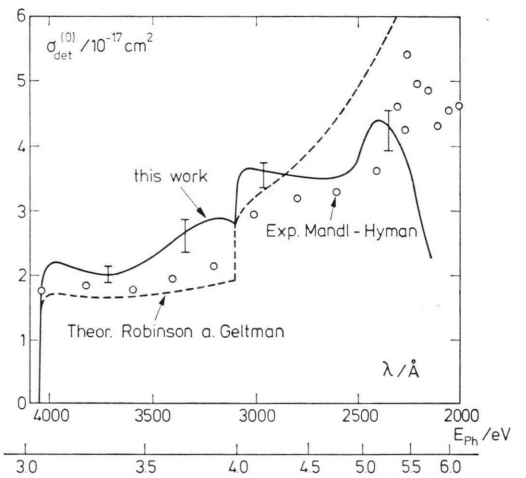

Fig. 9. Photodetachment cross-section of the I^- ground state.

The I^- photodetachment cross-section consists of two parts resulting from the processes where the final state neutral iodine atom is left in its $^2P^0_{3/2}$ or $^2P^0_{1/2}$ ground state ($\sigma_{\text{det}}^{(0)} = \sigma_{\text{det},1}^{(0)} + \sigma_{\text{det},2}^{(0)}$). Both contributions exhibit a vertical onset at their threshold energies 3.062 eV and 4.005 eV respectively. This is a direct consequence of Wigner's threshold law [25]

$$\sigma_{\text{det}} \sim (E_{\text{Ph}} - E_0)^{l+1/2}\,,$$

E_{Ph} = photon energy, E_0 = threshold energy, l = orbital angular momentum quantum number of free electron, because a bound p-electron is transferred to an unbound s-state in both cases.

The smooth rise of the cross-section, starting at approximately 3.3 eV is probably due to the transition that releases the free electron in a d-state. The threshold for this absorption process is, of course, also 3.062 eV, but due to its horizontal onset, it

does not contribute significantly before about 0.25 eV above threshold.

For an analysis of the cross section $\sigma_{det}^{(0)}$ beyond the second threshold at 4.005 eV, we extrapolate $\sigma_{det,1}^{(0)}$ qualitatively and subtract it from the total cross-section $\sigma_{det}^{(0)}$. Besides a sudden onset at 4.005 eV, the cross-section $\sigma_{det,2}^{(0)}$ resulting from this procedure exhibits a smooth rise at about 4.3 eV, and a very pronounced broad "line" centered at approximately 5.3 eV. The former feature can again be considered as a free d-electron contribution to the absorption process. The second, very strong feature, can be interpreted as arising from an absorption process from the I^- ground state to one or several unresolved compound states of the negative iodine ion, situated between the ground state and the first excited state of the neutral atom. By qualitative measurements at a microwave discharge, it was possible to show that this broad "line" disappears under conditions where the affinity continuum also disappears, but the diffuse molecular bands still being present. This is a very strong support for the interpretation given above. Performing absorption measurements at a CsI-plasma, Mandl and Hyman [7] found two peaks at 5.4 and 5.5 eV (see Fig. 9), which differs from our finding. However, as compound states may undergo autoionisation, this difference could well be attributed to differences in the population densities in their absorption and our emission experiment.

Possible compound states could arise from double excitation of outer-shell electrons (e. g. $5s^2\,5p^4\,6s\,6p$) or from excitation of an inner-shell electron as well (e. g. $5s\,5p^6\,6p$). Of course, no conclusions about the configuration of such a state can be drawn from the energy and halfwidth of the peak reported here. However, as Mandl and Hyman [7] remark, Henry performed unpublished calculations of double electron excitation states of the negative ions $F^-(2s^2\,2p^4\,3s\,3p)$ and Cl^- $(3s^2\,3p^4\,4s\,4p)$ and found their energies to be 14.35 eV and 9.16 eV respectively. Extrapolating these results to the I^- ion, an energy around 5.3 eV seems quite reasonable.

3. Analysis of the Visible and Infrared Continuum

The evaluation procedure is the same as described in Chapter 2.2. The measured spectral continuum intensities in the wavelength range from 0.4 to 1.9 μ at the plasma temperatures 6700, 6900, and 7070 K (see Fig. 5) are converted into absorption coefficients, using Kirchhoff's law.

3.1. Possibly Contributing Radiation Processes

According to the composition of the investigated iodine plasma (full dissociation, about 1% ionisation) we consider as possibly contributing radiation processes the following ones:

(a) an electron-ion continuum comprising free-free and free-bound transitions;

(b) an electron-atom continuum (so-called free-free-minus continuum);

(c) an affinity continuum due to a conceivable excited state of the I^- ion, analogous to the uv affinity continuum (see Chapter 2);

(d) an association continuum, resulting from radiative recombination of a neutral iodine atom with a positive ion to form a positive molecular I_2^+ ion;

(e) continua of highly excited states of the I_2 molecule (recombination and dissociation continua), which may still contribute despite full dissociation, as is shown by the still strong emission in the diffuse uv-bands (see Chapter 2.2).

3.2. Subtraction of the Electron-Ion Contribution

The only radiation process which contributes with certainty is the electron-ion continuum. As it is only of minor interest, the first step of the analysis will be its subtraction from the total continuum.

Considering first the wavelength range $\lambda > 1.25\ \mu$ (see Fig. 5) we choose the ansatz

$$\varkappa_{tot} = \varkappa_1 + \varkappa_2\,,$$

$\varkappa_1$ containing the electron-ion contribution and scaling with the square of electron density, $\varkappa_2$ describing the processes (b), (c), and (d), listed in Chapter 3.1, and scaling with the product of electron density and neutral atom density. This knowledge of the temperature dependence of $\varkappa_1$ and $\varkappa_2$ together with the experimentally determined quantities $\varkappa_{tot}$ and its temperature derivate $\partial\varkappa_{tot}/\partial T$, allows the determination of $\varkappa_1$ and $\varkappa_2$ for different wavelengths by solving two linear equations.

Approximating the absorption coefficient of the electron-ion continuum by the common expression, which describes free-free transitions and free-bound transitions of a quasi-continuum of energy levels,

and which accounts for deviations from a pure Coulomb field by a factor $\xi(\lambda)$, the above described procedure yields the following ξ-values:

$\lambda(\mu)$	1.9	1.7	1.5	1.3
ξ	2.75	3.25	3.60	3.75

These numbers show a considerable deviation of the e-I^+ potential from a Coulomb potential of a single positively charged ion. A comparison with the ξ-factors of the next element in the periodic system (Xe, $\xi = 2-3$, [28]) however shows, that these values are reasonable.

Thus the electron-ion continuum accounts for $50-70\%$ of the total continuum in the wavelength range from 1.3 to 1.9 μ. Assuming a constant factor $\xi = 3.8$ for shorter wavelengths, the contribution of this continuum is only about 20% in the range 1.2 to 0.4 μ.

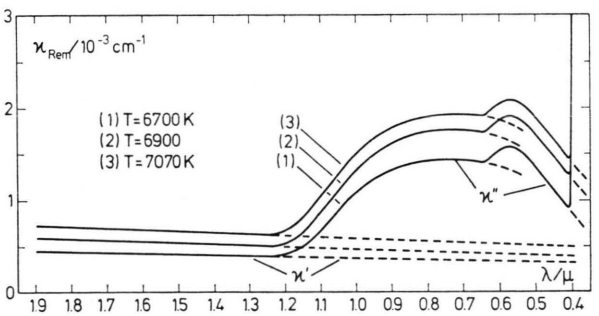

Fig. 10. Unknown contribution to the absorption coefficient of the iodine continuum.

Figure 10 shows the absorption coefficient $\varkappa_{Rem}$ after subtraction of the electron-ion contribution, as a function of wavelength for three different temperatures. Its characteristic features are two long wavelength thresholds near 0.64 and 1.25 μ. For further analysis, the absorption coefficient $\varkappa_{Rem}$ is separated by linear extrapolation as shown in Fig. 10 into two continua with and without threshold structure respectively:

$$\varkappa_{Rem} = \varkappa' + \varkappa'' .$$

3.3. Continuum $\varkappa'$ without Threshold Structure

A recombination or dissociation continuum can be excluded for this part of the continuum, because of its extension over a wide wavelength interval without exhibiting any characteristic features. Possibly contributing radiation processes are a free-free-minus continuum, an association continuum, and an affinity continuum. The temperature dependence of all three mechanisms scales very closely with the product of electron density and neutral atom density (see Chapter 3.2). The only distinctive features left are therefore the dependence on wavelength and the absolute value of the absorption coefficient compared with theoretical estimates.

The discussion of a contribution of free-free-minus radiation can be done most reliably and conveniently by comparing the absorption coefficient $\varkappa'$ to a theory of Kas'yanov and Starostin [29]. This theory relates the cross-section for emission of bremsstrahlung to the elastic electron-atom cross-section Q_{e-I}, which is approximately known for the iodine atom from quantum mechanical calculations of Robinson and Geltman [8]. Using an energy averaged cross-section $Q_{e-I} = 3 \times 10^{-15}\,cm^2$ a comparison of $\varkappa'$ to this theory at a temperature 6900 K yields the following result:

λ/μ	1.0	1.5	1.9
$\varkappa'_{exp}/10^{-4}\,cm^{-1}$	4.7	5.3	5.8
$\varkappa_{ffm}/10^{-4}\,cm^{-1}$	0.6	1.8	3.3

Although the magnitude of these numbers is of the same order, there is no similarity of their wavelength dependence at all. Therefore, it can be concluded that a significant contribution to $\varkappa'$ due to free-free-minus radiation does not exist below about 1.5 μ.

Another possible contribution to $\varkappa'$ is an association continuum of a neutral iodine atom and a positive iodine ion, both in its ground states initially, as illustrated in Figure 11 b. No comparison is possible in this case with a general theory, because none does exist, nor are data for the I_2^+ molecule available. However, an analogous radiation process is known in the case of hydrogen (H_2^+ continuum). It has been treated theoretically by Boggess [25], and Kruse and Popp [26] proved its existence experimentally. Following a suggestion of Mück and Popp [12], we compare the non-hydrogenic absorption coefficient $\varkappa'$ of this experiment with the H_2^+ continuum. This can be conveniently done by using a function $F(\lambda, T)$ introduced by Boggess [25]. A conversion of the absorption coefficient $\varkappa'$ into the function $F_{I_2^+}$ yields the same temperature and

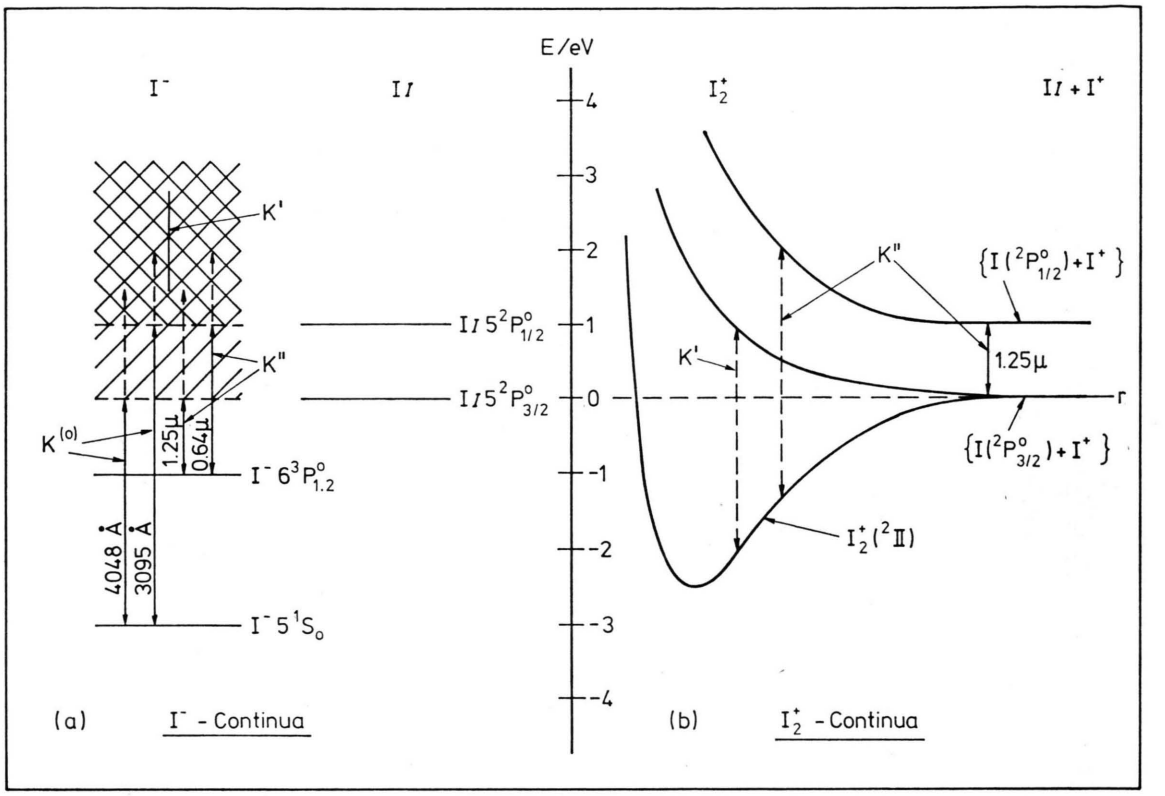

Fig. 11. Analysis of the unknown part of the iodine continuum. ($K^{(0)}=\varkappa^{(0)}$; $K'=\varkappa'$; $K''=\varkappa''$).

wavelength dependence as exhibited by $F_{H_2^+}$, if $\varkappa'$ is decreased by the theoretical absorption coefficient for a free-free-minus continuum (see above). No coincidence however exists in the order of magnitude. At $\lambda = 1.5\,\mu$ for example, the comparison yields:

$$F_{I_2^+} = 50 \cdot F_{H_2^+}.$$

The function $F(\lambda, T)$ involves the properties of the molecular ions H_2^+ and I_2^+, which will, of course, be rather different. The internuclear distance enters with the second power and will increase $F_{I_2^+}$ considerably. Another important parameter is the ratio of the statistical weights of the initial states, which can radiate, to that of all initial states. Heavy molecules like I_2^+ exhibit more energy states and less severe selection rules, facts that will also increase $F_{I_2^+}$. These and other differences may be responsible for an enhancement of the F function for the I_2^+ molecule. Together with the excellent fit of the wavelength dependence, an interpretation of $\varkappa'$ as an association continuum is possible.

As a third possible contribution to $\varkappa'$ an affinity continuum of a stable, excited state $I^{-(*)}$ of the negative iodine ion shall be investigated. The onset of such an affinity continuum would be situated beyond $\lambda = 1.9\,\mu$, because $\varkappa'$ does not exhibit any long wavelength threshold in the range covered by this experiment. This yields a binding energy smaller than 0.65 eV, i. e. an excitation energy larger than 2.4 eV for such an $I^{-(*)}$-state. For this interpretation to be consistent, a detachment cross-section $\sigma_{det}^{(*)}$ independent of temperature must result from the absorption coefficients $\varkappa'$:

$$\sigma_{det}^{(*)}(\lambda) = \varkappa(\lambda, T)/n_-^{(*)}(T)$$

$n_-^{(*)}$ = population density of the assumed $I^{-(*)}$ state. As the excitation energy $E^{(*)}$ is very close to the electron affinity, the temperature dependence of $n_-^{(*)}$ scales nearly with the product of electron and neutral atom density. This indeed yields a temperature independent cross-section $\sigma_{det}^{(*)}$. Choosing $E^{(*)} = 3$ eV and a statistical weight $g^{(*)} = 1$, a cross-section $\sigma_{det}^{(*)} = 6 \times 10^{-16}\,cm^2$ results at $\lambda = 1.5\,\mu$,

which is about a factor of 30 stronger than the photodetachment cross-section of the I^- ground state. It can therefore be concluded that no affinity continuum contributes significantly to the absorption coefficient $\varkappa'$.

The main radiation processes responsible for $\varkappa'$ seem to be an association continuum due to the I_2^+-molecule for $\lambda < 1.5\,\mu$ and both this and a free-free-minus continuum in the range $1.5\,\mu < \lambda < 1.9\,\mu$. For still longer wavelengths, the latter will probably dominate.

3.4. Continuum $\varkappa''$ with Threshold Structure

The two long wavelength thresholds $\lambda_1 = 1.25\,\mu$ and $\lambda_2 = 0.64\,\mu$ correspond to photon energies $E_{\mathrm{Ph},1} = 0.99$ eV and $E_{\mathrm{Ph},2} = 1.94$ eV. The smooth threshold character introduces rather large uncertainties in both cases:

$$\Delta\lambda_1 = +0.07\,\mu \rightarrow \Delta E_{\mathrm{Ph},1} = -0.05\ \mathrm{eV},$$
$$\Delta\lambda_2 = +0.02\,\mu \rightarrow \Delta E_{\mathrm{Ph},2} = -0.06\ \mathrm{eV}.$$

Radiation processes contributing to $\varkappa''$ must therefore involve potential energy curves with minimum energy differences in the range 0.94 to 0.99 eV and 1.88 to 1.94 eV respectively. Possible mechanisms are again an affinity continuum of an excited $I^{-(*)}$-ion, an association continuum due to the I_2^+-molecule, or an I_2 molecular continuum. Distinctive features for the following analysis are the dependence on wavelength and temperature and the magnitude of the absorption coefficient.

The energy difference of the two thresholds $E_{\mathrm{Ph},2} - E_{\mathrm{Ph},1} = (0.95 \pm 0.05)$ eV coincides within the given uncertainty range with the neutral iodine atom ground state splitting $\Delta E = 0.94$ eV. It is therefore tempting to investigate the possibility of an affinity continuum due to an excited $I^{-(*)}$ ion, analogous to the uv affinity continuum (see Figure 11 a). The first onset $\lambda_1 = 1.25\,\mu$ yields a binding energy $E_B^{(*)} = 0.99$ eV of such a state, which corresponds to an excitation energy of $E^{(*)} = EA - E_B^{(*)} = 2.07$ eV above the I^- ground state. Calculating a photodetachment cross-section $\sigma_{\mathrm{det}}^{(*)}$ from the three absorption coefficients $\varkappa''$ by simply dividing the latter by the population densities $n_-^{(*)}$ of such an excited state indeed yields a temperature independent quantity of reasonable magnitude. The smooth threshold onsets indicate that the unbound state of the radiating electron will be a p-state (see Chapter 2.3), from which follows, that the corresponding discrete state is a s or a d one. Performing an isoelectronic extrapolation from Cs^+ via Xe^0 to I^- one can show that the bound electron will most probably accupy a 6s-state (the 5d series yields an energy higher than the electron affinity). The electron configuration of the assumed $I^{-(*)}$ ion will therefore be $5s^2\,5p^5\,6s$, $^3P^0_{2,1}$. The dashed line in Fig. 12 shows the detachment cross-section $\sigma_{\mathrm{det}}^{(*)}$, calculated with the assumption that $\varkappa''$ represents such an affinity continuum alone and using the statistical weight $g_-^{(*)} = 8$ of this $I^{-(*)}$ state. As the ratio of the statistical weights of the two $^2P^0$ ground levels of the neutral iodine atom is 2:1, the two parts of this affinity continuum, whose thresholds are λ_1 and λ_2 respectively, should contribute with this same ratio. The solid line in Fig. 12 shows the detachment cross-section $\sigma_{\mathrm{det}}^{(*)}$ following from this argument. Figure 12 also shows that about half of the absorption coefficient $\varkappa''$ can be interpreted as an affinity continuum due to an excited negative iodine ion.

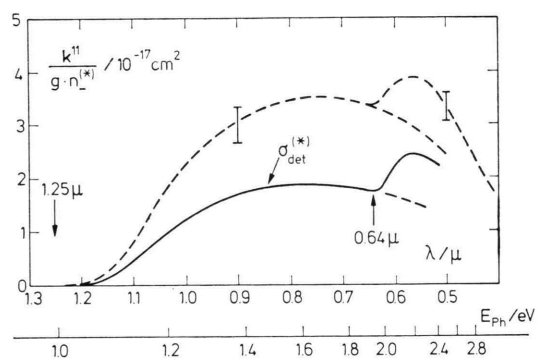

Fig. 12. Photodetachment cross-section of a proposed excited I^- state ($\varkappa''$ instead of k^{11}).

The assumption of $\varkappa''$ being an association continuum of a neutral iodine atom in the state $^2P^0_{1/2}$ and a positive iodine ion in its ground state is also consistent with the long wavelength threshold at $\lambda_1 = 1.25\,\mu$. Figure 11 b shows a schematic diagram of this radiation process. The calculation of its temperature dependence yields a result close to that shown by $\varkappa''$. Unfortunately, no theoretical estimates of its absolute magnitude are possible. Again, the only possibility is a comparison with the H_2^+ continuum. The evaluation of the relevant function $F_{I_2^+}$ (see Chapter 3.2) yields values that are by a factor of about 500 larger than those of $F_{H_2^+}$. It is unclear to what extent considerable differences of

the potential energy diagrams, radiation selection rules, and transition probabilities between the I_2^+ and H_2^+ molecular ions may be responsible for this factor.

Finally, the principal possibility of continua of the I_2 molecule contributing to the absorption coefficient $\varkappa''$ will be mentioned. The following recombination continua

$$I(^2P^0_{3/2}) + I(^2P^0_{1/2}) \rightarrow I_2(^1\Sigma_g^+) + h\,c/\lambda\,, \qquad (1)$$

$$I(^2P^0_{1/2}) + I(^2P^0_{1/2}) \rightarrow I_2(^1\Sigma_g^+) + h\,c/\lambda \qquad (2)$$

would exhibit long wavelength thresholds at λ_1 and λ_2. The I_2 potential energy diagram [30], however, contains no possible radiation transitions that could also explain the wide wavelength range and the temperature dependence of $\varkappa''$.

The author's conclusion is that the dominant contributions to the absorption coefficient $\varkappa''$ are an affinity continuum of an excited state of the I^--ion and an association continuum due to the I_2^+ molecule. Both continua exhibit thresholds at λ_1, but only the former one a second threshold at λ_2.

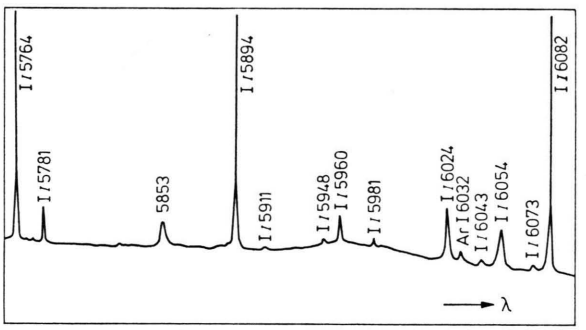

Fig. 13. Photoelectric recording of the iodine arc near 6000 Å (wavelengths in Å).

3.5. *Excited I^- State*

The interpretation of a considerable part of the visible and near infrared iodine continuum due to radiation processes associated with the negative iodine ion results in the energy level diagram of Figure 11 a. Hence, the question arises about a line transition between the levels $^3P_1{}^0$ and $^1S_0$, which should be found in the wavelength range between 5840 and 6000 Å. A photoelectric recording of the spectrum in this region is shown in Figure 12. All spectral lines have been identified [24] with exception of the line at 5853 Å. An investigation of its dependence on temperature shows an increase weaker than that of I_I lines, but stronger than one would expect for such an I^- line. Additional trials to find this line with a CsI plasma of high negative ion density also could not find it [31]. However, it is unclear whether this excludes the existence of such an excited I^- state. Of special importance in this respect is the question of how strong the $\Delta S = 0$ selection rule suppresses the transition. On the other hand, double negatively charged iodine ions have been observed by mass spectrometer methods [32], a fact that indicates that the I^- ion field is even strong enough to bind a second electron. From this point of view, the existence of an excited I^- state would be consistent.

4. Summary

The continuum radiation which is emitted along the axis by a low current arc operated in pure iodine vapour at atmospheric pressure has been quantitatively measured and discussed. The ultraviolet wavelength region is dominated by the affinity continuum of the I^- ground state. From this an electron affinity of the neutral iodine atom of 3.062 eV and the photodetachment cross-section of the negative iodine ion as a function of photon energy is derived. The latter exhibits a resonance structure near 5.3 eV, which is attributed to an absorption process from the I^- ground state to a compound state above the detachment limit.

The visible and infrared continuum exhibits two long wavelength thresholds near 1.25 μ and 0.64 μ. Subtraction of the electron-ion contribution leaves a residual continuum which constitutes in the visible and near infrared region about 80%, at 1.9 μ about 30% of the total continuum. An analysis according to intensity, dependence on wavelength and temperature, threshold energy and threshold structure, suggest the contribution of two dominant radiation processes: a second affinity continuum due to an excited state of the I^- ion about 2 eV above its ground level and an association continuum of I_2^+ molecules. Contrary to former interpretations, electron-atom bremsstrahlung is negligible in the visible range. Its contribution becomes significant only for $\lambda > 1.5\ \mu$.

Acknowledgements

The author wishes to thank Prof. H. Maecker for suggesting and steadily promoting this investigation,

and Prof. H.-P. Popp and Dr. G. Mück for their continuous interest and many invaluable discussions.

Financial support for part of this work by the Deutsche Forschungsgemeinschaft is also gratefully acknowledged.

[1] H.-P. Popp, 8. Intern. Conf. Phen. Ionized Gases, Springer-Verlag, Wien 1967, S. 448.
[2] H.-P. Popp, Z. Naturforsch. **22 a**, 254 [1967].
[3] G. Mück u. H.-P. Popp, Z. Naturforsch. **23 a**, 1213 [1968].
[4] H. Frank, M. Neiger u. H.-P. Popp, Z. Naturforsch. **25 a**, 1617 [1970].
[5] A. Mandl, Phys. Rev. A **3**, 251 [1971].
[6] D. E. Rothe, Phys. Rev. **177**, 93 [1969].
[7] A. Mandl u. H. A. Hyman, Phys. Rev. Lett. **31**, 7, 417 [1973].
[8] E. J. Robinson u. S. Geltman, Phys. Rev. **153**, 4 [1967].
[9] H. A. Kramers, Phil. Mag. **46**, 836 [1923].
[10] A. Unsöld, Ann. Phys. **33**, 607 [1938].
[11] H. Maecker u. Th. Peters, Z. Phys. **139**, 448 [1954].
[12] G. Mück, 11th Intern. Conf. Phen. Ionized Gases, Prag 1973, p. 231.
[13] G. Mück u. H.-P. Popp, Z. Naturforsch. **28 a**, 1964 [1973].
[14] J. Euler, Ann. Phys. **6**, 11 [1953].
[15] H. Magdeburg, Z. Naturforsch. **20 a**, 980 [1965].
[16] E. Pitz, Appl. Opt. **10**, 4, 813 [1971].
[17] W. Frie, Z. Physik **201**, 269 [1967].
[18] G. Herzberg, Spectra of Diatomic Molecules, D. van Nostrand Comp., Amsterdam 1966.
[19] Ch. E. Moore, Atomic Energy Levels, Nat. Bur. Stand. Circ. 467 [1949].
[20] D. R. Bates u. A. Damgaard, Phil. Trans. Roy. Soc. **A 242**, 101 [1949].
[21] H. Friedrich, K. Katterbach u. E. Trefftz, JQSRT **10**, 11 [1970].
[22] R. S. Berry, C. W. Reimann u. G. N. Spokes, J. Chem. Phys. **37**, 2278 [1962].
[23] R. K. Asundi u. P. Ventkateswarlu, Ind. J. Phys. **21**, 101 [1947].
[24] C. C. Kiess u. Ch. H. Corliss, J. Res. Nat. Bur. Stand. **63 A**, 1 [1959].
[25] E. P. Wigner, Phys. Rev. **73**, 1002 [1948].
[26] A. Boggess, Astrophys. J. **129**, 432 [1959].
[27] S. Kruse u. H.-P. Popp, to be published.
[28] D. Schlüter, Z. Astrophys. **61**, 67 [1965].
[29] V. Kas'yanov u. A. Starostin, Sov. Phys. JETP **21**, 193 [1965].
[30] R. S. Mulliken, J. Chem. Phys. **55**, 288 [1971].
[31] P. Lukas, private communication.
[32] H. Bauman et alias, Nucl. Instr. Meth. **95**, 389 [1971].